Comparative Biochemistry and Physiology, Part A 282 (2023) 111443

Contents lists available at ScienceDirect

Comparative Biochemistry and Physiology, Part A

journal homepage: www.elsevier.com/locate/cbpa

Hypoxia acclimation improves mitochondrial efficiency in the aerobic swimming muscle of red drum (*Sciaenops ocellatus*)

Kerri Lynn Ackerly [a,*], Benjamin Negrete Jr [a], Angelina M. Dichiera [b], Andrew J. Esbaugh [a]

[a] Marine Science Institute, The University of Texas at Austin, Port Aransas, TX 78373, USA
[b] Department of Zoology, The University of British Columbia, Vancouver, British Columbia V6T 1Z4, Canada

ARTICLE INFO

Edited by Michael Hedrick

Keywords:
Oxidative phosphorylation
Fish
Heart
Red muscle
Low oxygen

ABSTRACT

Environmental hypoxia (low dissolved oxygen) is a significant threat facing fishes. As fishes require oxygen to efficiently produce ATP, hypoxia can significantly limit aerobic capacity. However, some fishes show respiratory flexibility that rescues aerobic performance, including plasticity in mitochondrial performance. This plasticity may result in increased mitochondrial efficiency (e.g., less proton leak), increased oxygen storage capacity (increased myoglobin), and oxidative capacity (e.g., higher citrate synthase activity) under hypoxia. We acclimated a hypoxia-tolerant fish, red drum (*Sciaenops ocellatus*), to 8-days of constant hypoxia to induce a hypoxic phenotype. Fish were terminally sampled for cardiac and red muscle tissue to quantify oxidative phosphorylation, proton leak, and maximum respiration in tissue from both hypoxia-acclimated and control fish. Tissue was also collected to assess the plasticity of citrate synthase enzyme activity and mRNA expression for select oxygen storage and antioxidant pathway transcripts. We found that mitochondrial respiration rates were not affected by hypoxia exposure in cardiac tissue, though citrate synthase activity and myoglobin expression were higher following hypoxia acclimation. Interestingly, measures of mitochondrial efficiency in red muscle significantly improved in hypoxia-acclimated individuals. Hypoxia-acclimated fish had significantly higher OXPHOS Control Efficiency, OXPHOS Capacity and Coupling Control Ratios (i.e., LEAK/OXPHOS). There was no significant change to citrate synthase activity or myoglobin expression in red muscle. Overall, these results suggest that red muscle mitochondria of hypoxia-acclimated fish more efficiently utilize oxygen, which may explain previous reports in red drum of improved aerobic swimming performance in the absence of improved maximum metabolic rate following hypoxia acclimation.

1. Introduction

Hypoxia (low dissolved oxygen (O_2)) is currently considered one of the most significant threats facing marine fishes (e.g., Diaz, 2001; Rabalais and Turner, 2019; Schmidtko et al., 2017). Hypoxic dead zones are especially prevalent in coastal areas with significant eutrophication (e.g., The Gulf of Mexico) and have been increasing in size and duration for decades (e.g., Diaz and Rosenberg, 2008), making it increasingly difficult for species to avoid these unfavourable habitats. As a result, it is important for species in these affected areas to be able to persist under chronic hypoxia.

O_2 is essential for sustainable aerobic ATP production within the mitochondria, the primary site of O_2 consumption (reviewed by Pamenter, 2014). Thus, hypoxia can significantly limit aerobic metabolic capacity of fishes by imposing limits on the mitochondria's capacity for ATP production (Buck and Pamenter, 2006; Sokolova et al., 2019). Within the mitochondria, O_2 acts as the terminal electron receptor within the electron transport chain. This results in the movement of protons across the mitochondrial membrane to create an electrochemical gradient that drives ATP production via ATP synthase (oxidative phosphorylation, OXPHOS). The relationship between the movement of protons and ATP production can vary because of mitochondrial proton leak (LEAK), the movement of protons across the mitochondrial membrane not tied to ATP synthesis, and can affect the efficiency of mitochondria (i.e., a higher LEAK rate can impair the gradient driving ATP synthesis) (reviewed by Brand, 2005).

Under hypoxia, fishes often undergo metabolic suppression to lessen O_2 demand (see review by Chapman and Mckenzie, 2009). Farhat et al. (2021) investigated mechanisms driving metabolic suppression in goldfish (*Carassius auratus*) following 4 weeks of chronic hypoxia and

* Corresponding author.
E-mail address: klackerly@utexas.edu (K.L. Ackerly).

https://doi.org/10.1016/j.cbpa.2023.111443
Received 16 March 2023; Received in revised form 11 May 2023; Accepted 13 May 2023
Available online 16 May 2023

overall found significant decreases in mitochondrial density across tissues, but changes to mitochondrial respiration rates were specific to tissue type and metabolic fuel. For example, there were no significant changes to OXPHOS or LEAK in cardiac or red muscle tissues, but a significant increase in LEAK in the liver tissue, and both OXPHOS and LEAK in brain tissue (Farhat et al., 2021). Interestingly, Hickey et al. (2012) found that acute hypoxia affected cardiac mitochondria differently based on the hypoxia tolerance of a species. They showed maintenance of OXPHOS under hypoxia in the hypoxia-tolerant epaulette shark (*Hemiscyllum ocellatum*), but in the hypoxia-sensitive shovelnose ray (*Aptychotrema rostrata*) demonstrated that OXPHOS was reduced by 50% under hypoxia. These data highlight the species- and tissue-specific nature of mitochondrial plasticity and the potential importance of a species' hypoxia tolerance.

Previous work in red drum (*Sciaenops ocellatus*), an economically important species found within dead zones in the Gulf of Mexico (Levin et al., 2009), has demonstrated significant hypoxia-induced respiratory plasticity that improved performance in hypoxic environments. Pan et al. (2017) showed that hypoxia-acclimated red drum reduced hypoxia vulnerability by significantly decreasing their critical oxygen thresholds (P_{crit}) – the oxygen tension below which a fish can no longer maintain resting oxygen demand. Negrete Jr et al. (2022) showed that after 8d of constant hypoxia red drum significantly increase haematocrit (Hct; % of red blood cells in whole blood), dynamically regulate the haemoglobin (Hb) pool to increase O_2-binding affinity and reduce pH sensitivity (i.e., Root effect), and improve maximum metabolic rates under hypoxia. Dichiera et al. (2022) showed hypoxia-acclimated red drum improve critical swimming speed when tested under normoxia compared to control fish, with changes likely owing to the capacity for anaerobic energy production since hypoxia-acclimated fish utilized significantly more burst swimming during swim trials. However, the effects of chronic hypoxia exposure on mitochondria and the role of mitochondrial plasticity in augmenting physiological performance in hypoxic environments has yet to be assessed in red drum.

On this background, the goal of this study was to determine the effects of chronic sub-lethal hypoxia exposure on mitochondrial performance and efficiency of red drum. To test this, we acclimated fish to chronic sub-lethal hypoxia (~30% air-saturation / ~6.17 kPa) for 8d. This O_2 level was chosen as it is above the P_{crit} for red drum (Ackerly and Esbaugh, 2020, 2021; Negrete and Esbaugh, 2019; Pan et al., 2017) and has been shown to induce a hypoxic phenotype (previously defined by Dichiera et al., 2022; Negrete Jr et al., 2022) within this species. Following acclimation, we assessed mitochondrial performance of two aerobic, energetically demanding tissues – cardiac muscle and red muscle. We also tested transcriptional regulation of myoglobin (*mb*), a gene important for oxygen storage and facilitated diffusion, and citrate synthase (*cs*), which is the rate-limiting step within the citric acid cycle that feeds substrates into the electron transport chain in the mitochondria and can be a marker for mitochondrial abundance. Additionally, we measured citrate synthase enzyme activity as a marker of mitochondrial abundance and quantified Hct to assess capacity for O_2 transport. In general, we hypothesized hypoxia-acclimated fish would maximize O_2 utilization within mitochondria by improving electron transport chain efficiency. More specifically, we predicted red muscle and cardiac muscle in hypoxia-acclimated fish would exhibit: decreased LEAK respiration rates; improved mitochondrial efficiency; increased myoglobin expression; and increased Hct; and/or decreased oxidative capacity (e.g., expression and activity of citrate synthase).

2. Methods

2.1. Experimental animals

All experimental protocols were approved by the University of Texas at Austin Institutional Animal Care and Use Committee (AUP-2018-00231; AUP-2021-00204). The red drum (*Sciaenops ocellatus*; Linnaeus 1766) included in this study were purchased from Ekstrom Aquaculture, LLC (Palacios, TX, USA). Fish were housed in 250 L tanks with recirculating filtered sea water from the Corpus Christi ship channel at the Fisheries and Mariculture Laboratory (FAML) at The University of Texas at Austin Marine Science Institute (Port Aransas, TX, USA). Fish were fed commercial fish pellets (Purina Animal Nutrition, LLC, USA) ad libitum daily except during the 48 h before sampling. Tanks were maintained at 24.7 ± 0.03 °C (average ± s.e.m.) at 30 ± 3 ppt on a 14 h light: 10 h dark photoperiod and were siphoned daily to remove debris.

2.2. Gene expression

These data were collected in tandem with Dichiera et al. (2022) and Negrete Jr et al. (2022), which focused on the plasticity of tissue oxygen extraction mechanisms and oxygen uptake mechanisms, respectively. Juvenile red drum were exposed to control normoxia ($n = 33$, mass: 64.8 ± 2.7 g, DO: 100.0 ± 0.1% air saturation (AS) / 20.58 kPa, pH: 8.02 ± 0.01) or chronic hypoxia ($n = 35$, mass: 61.9 ± 2.0 g, DO: 33.3 ± 0.2% AS / 6.85 kPa, pH: 8.10 ± 0.01) for 6 weeks (wk). Hypoxic conditions were established and maintained by bubbling nitrogen gas controlled by Oxy-Reg systems (Loligo® Systems) into tanks partially covered by bubble wrap to prevent surface mixing. Three replicate tanks were established for normoxic and hypoxic conditions, and fish were equally divided into and sampled among tanks at each time point (1d, 4d, 8d, 2wk, or 6wk; n = 6–8 per treatment at each time point). Details of sampling methods, mRNA isolation, and cDNA synthesis for heart and red muscle tissues are detailed in Dichiera et al. (2022). For the purposes of this study only samples from time points 1d, 4d, and 8d were used.

Maxima SYBR green / ROX qPCR Master Mix (Thermo Scientific) were used to perform qPCR analyses. Primer pairs used in this study (see Table 1) were designed based on predicted sequences from closely related Sciaenidae species (e.g., *Larimichthys crocea*) or from published red drum sequences when available. Standard curves were established for each primer pair using a two-fold dilution series of cDNA. mRNA expression of *mb* and *cs* were quantified in both cardiac (ventricle) and red muscle tissues using the following protocol: an initial denaturing temperate of 95 °C for 10 min; 40 cycles of 95 °C for 30s, 60.8 °C for 1 min, 72 °C for 30s; and a final cycle of 95 °C for 1 min, 30s at 55 °C, and 30c at 95 °C. Negative (nuclease-free molecular water) controls and no reverse transcriptase (no-RT) controls were performed with each gene. Expression of each gene was normalized to elongation factor 1 alpha (*ef1α*) (Watson et al., 2014), an appropriate house-keeping gene in fishes (e.g., Jorgensen et al., 2006; Yang et al., 2013). Raw ct values for *ef1α* were unaffected by hypoxia acclimation and did not change with time point. Expression for each gene was calculated relative to normoxic expression levels for each time point. Calculations were performed using the modified delta-delta Ct method (Pfaffl, 2001).

2.3. Mitochondrial performance

A second group of red drum were acclimated to chronic normoxia or hypoxia (normoxia: $n = 14$, mass: 58.1 ± 4.6 g, DO: 99.9 ± 0.3% AS / 20.56 kPa, pH: 8.06 ± 0.01; hypoxia: n = 14, mass: 69.7 ± 5.6 g, DO: 31.8 ± 0.3% AS / 6.54 kPa, pH: 7.85 ± 0.01) for 8 d, as described above,

Table 1
Real-time qPCR primer sequences to look at the effects of hypoxia acclimation on cardiac and red muscle tissues of red drum (*Sciaenops ocellatus*). Sequences are written 5′ to 3′. Reverse primers are genetic sequence complements.

Gene	Orientation	Sequence	Accession No
ef1α	F	GTCCGTGACATGAGGCAGACTG	**KJ958539**
	R	GTTGCTGGATGTCCTGCACG	
cs	F	TGTCACCATGCTGGATAACTTC	**OP937329**
	R	TCTTGTGGACACCCTCAGAGTA	
mb	F	CTGAAGTTTTCAAGGGGGATCT	**OP999039**
	R	CCAAGTTTTCTGGCAAGTCTTC	

and sampled for heart tissue. A third group of red drum were acclimated to chronic normoxia or hypoxia (normoxia: $n = 12$, mass: 768.3 ± 61.6 g, DO: 98.0 ± 1.7% AS / 20.17 kPa, pH: 7.8 ± 0.07; hypoxia: n = 12, mass: 670.6 ± 46.9 g, DO: 33.8 ± 3.7% AS / 6.96 kPa, pH: 7.7 ± 0.1) for 8 d, as described above, and sampled for red muscle tissue. Two separate acclimations were performed for cardiac and red muscle because during the initial trial we discovered larger fish were needed for sufficient tissue for red muscle mitochondrial analyses. Note that both fish sizes would be considered the juvenile life stage, and no direct comparisons were made between red muscle and cardiac tissue. The 8d time point was chosen as previous data (see Dichiera et al., 2022; Negrete Jr et al., 2022) show red drum exhibit a hypoxic phenotype by 8d of exposure, as evidenced by increased maximum metabolic rate in hypoxia, lower critical oxygen threshold, higher critical swim speed, and higher Hb-O_2 binding affinity.

To assess mitochondrial performance of cardiac and red muscle tissues, individuals were euthanized with an overdose of 500 mg L^{-1} tricaine methanesulfonate (MS-222) buffered with 1 g L^{-1} sodium bicarbonate and a spinal transection. Prior to dissection, blood was sampled via caudal puncture, loaded into micro-capillary tubes, and centrifuged at 12,000 *G* for 2 min to quantify Hct in triplicate. Individuals subsequently had either the whole heart (acclimation group 2) or a strip of red muscle tissue (acclimation group 3) from the left lateral side immediately dissected. The aorta, bulbous arteriosus, connective tissues, and the atrium were removed from the heart to isolate the ventricle. The ventricle was then weighed to calculate relative ventricular mass (ventricle mass (mg) / total mass of the individual (g)) and the ventral half was carefully dissected for homogenization. The red muscle tissue was ensured to have no remnants of white muscle attached prior to homogenization. Tissues were gently blotted on a clean Kimwipe™ before 11.5 mg of heart and 10 mg red muscle were weighed on a balance with 0.1 mg precision (Denver Instruments, Inc., NY, USA) for homogenization. Remaining tissue not used for homogenization was kept at −80 °C for citrate synthase enzyme activity measures (described below).

Following dissection and weighing, tissues were immediately placed in 500 μL ice cold MiR05 solution (0.5 mM EGTA, 3 mM $MgCl_2$, 60 mM lactobionic acid, 20 mM taurine, 10 mM KH_2PO_4, 20 mM HEPES, 110 mM D-sucrose, buffered to pH 7.0 using 5 M KOH) and gently homogenized on ice using a 7 mL glass Dounce homogenizer (Wheaton, USA). Homogenates were immediately transferred to an Oroboros Oxygraph-2 k respirometer system (Oroboros Instruments, Innsbruck, Austria) test chamber (2.2 mL total volume of MiR05 + homogenate, 24 °C) to quantify O_2 consumption of mitochondria. Oxygen consumption of the tissues was quantified as mass-specific O_2 flux (pmol O_2 s^{-1} mg^{-1}) in real time using DatLab, Version 7 (Oroboros Instruments, Innsbruck, Austria). A modified substrate-uncoupler-inhibitor-titration (SUIT) protocol (Fig. 1) was performed to assess mitochondrial performance and efficiency following Johansen and Esbaugh (2017). Briefly, the following titration sequence was used: 1) 280 U/mL catalase and 3 μL 3% H_2O_2 to increase chamber to 200% AS to prevent O_2 limitations from affecting mitochondrial performance; 2) 2 mM malate, 5 mM pyruvate, 10 mM glutamate to provide substrates for Complex I (CI) without ADP; 3) 1 mM steps of ADP until saturation to induce CI-OXPHOS; 4) 10 μM cytochrome *c* to assess mitochondrial membrane integrity; 5) 10 mM succinate as substrate for Complex II (CII) and 1 mM of ADP to induce maximal respiration (OXPHOS; State 3 (Chance and Williams, 1955)); 6) 5 nM oligomycin to inhibit F_0F_1-ATPase (ATP synthase) to measure LEAK (State 4 (Chance and Williams, 1955)); 7) 0.25 μM carbonyl cyanide p-(trifluoro-methoxy) phenyl-hydrazone (FCCP) steps to saturation to measure uncoupled electron transport capacity (ETS; State 3u (Chance and Williams, 1955)); 8) 0.5 μM rotenone to inhibit CI to assess contribution of CII to ETS and determine the CI and CII uncoupled ratios; 9) 2.5 μM antimycin a to assess residual background cellular oxygen consumption (ROX) by inhibiting OXPHOS. At the completion of each experiment, test chambers were emptied and cleaned using the following protocol: 5 min rinse with DI water, 20 min rinse with proofed yeast, 3 × 5 min rinses with DI, 3 × 5 min with 70% EtOH.

Oxygen consumption (i.e., raw respiration rates) of each step is reported as mass-specific O_2 flux (pmol O_2 s^{-1} mg^{-1}). With these data, we calculated OXPHOS Capacity (OXPHOS-LEAK) to assess coupled respiration above LEAK; ETS Capacity (ETS-LEAK) to assess uncoupled respiration above LEAK; and Excess Capacity (ETS-OXPHOS) to assess uncoupled respiration above coupled respiration. To assess the efficiency of OXPHOS relative to LEAK, we calculated the OXPHOS Control Efficiency ((OXPHOS-LEAK)/OXPHOS) and the Respiratory Control Ratio (RCR) (OXPHOS/LEAK). Control ratios (CR) were also calculated for the following measures: OXPHOS CR (OXPHOS/ETS; ratio of ETS used by OXPHOS); LEAK CR (LEAK/ETS; ratio of ETS driven by LEAK); CI Coupled CR (CI/OXPHOS; ratio of OXPHOS driven by CI); CI Uncoupled CR (CI_{UC}/ETS; ratio of ETS driven by CI). To calculate CI_{UC}, we first calculated a CII_{UC} ratio from the mass-specific O_2 flux following the addition of rotenone in the protocol described above and then subtracted this value from 1 to assess the contribution of CI. All mitochondrial performance measures (raw respiration rates, capacities, and CRs) were assessed and reported as ROX-corrected values.

Due to inconsistency with FCCP in some cardiac muscle samples, a portion of the data have been excluded. In a subset of these cardiac muscle samples, addition of FCCP did not bring oxygen consumption measures within a level consistent with what was achieved at OXPHOS. Therefore, ETS measurements were deemed unreliable if oxygen consumption measurements following FCCP titration did not reach or

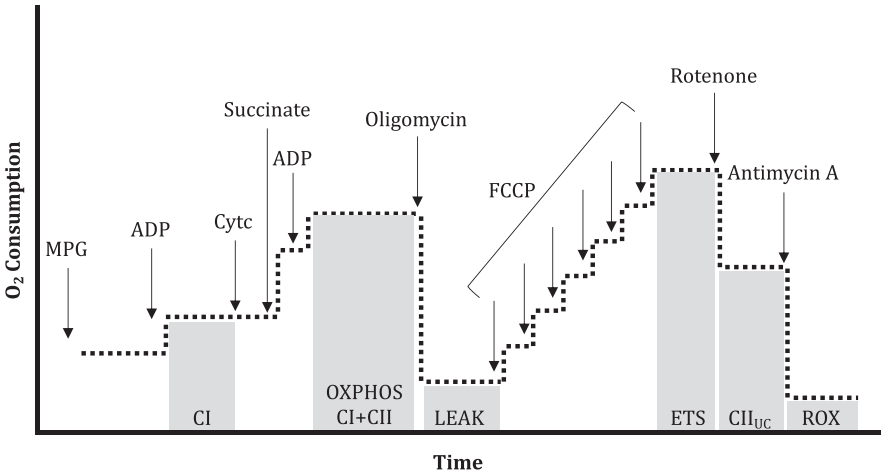

Fig. 1. Schematic of the substrate-uncoupler-inhibitor titration (SUIT) protocol used to assess mitochondrial respiration in both cardiac and red muscle tissues. This figure is adapted from Johansen and Esbaugh (2017). The protocol is performed as follows, with grey boxes indicating the respiration states measured at each step: malate, pyruvate, and glutamate (MPG) and ADP are added to stimulate Complex I (CI). Cytochrome C (Cytc) is then added to assess membrane integrity. Complex II (CII) is then stimulated via the addition of succinate and ADP to measure oxidative phosphorylation (OXPHOS). Oligomycin, which inhibits F_0F_1-ATPase (ATP synthase), is added to assess LEAK respiration. FCCP is then added to saturation to assess ETS. Rotenone is then added to inhibit CI to assess CII uncoupled respiration. Antimycin A is added to inhibit OXPHOS and assess background oxygen consumption (ROX). (For interpretation of the references to colour in this figure legend, the reader is referred to the web version of this article.)

exceed 95% of OXPHOS. Therefore, ETS measurements for the cardiac tissue have reduced sample sizes (normoxia: $n = 6$; hypoxia: $n = 9$).

As mentioned above, mitochondrial membrane integrity was assessed by adding cytochrome *c* following the induction of CI-OXPHOS and prior to the induction of OXPHOS. We calculated the percent (%) change in respiration between CI-OXPHOS and the addition of cytochrome *c*. While there was no significant change following the addition of cytochrome *c* in cardiac tissue preparations (normoxia: 0.14 ± 2.79%; hypoxia: 2.5 ± 2.73%), red muscle tissue preparations did show increased respiration rates following the addition of cytochrome *c* (normoxia: 26.97 ± 4.42%; hypoxia: 32.59 ± 4.09%). While this suggests that the red muscle preparation suffered from some loss of outer membrane integrity, it is important to note that there was no difference in the percent change between experimental treatments (*t*-test $p = 0.36$), and respiration values were comparable to prior work in red drum red muscle (Johansen and Esbaugh, 2017).

2.4. Citrate synthase activity

Citrate synthase enzyme activity assays were performed on remaining ventricle and red muscle tissues (see above). Tissues were ground to powder over liquid nitrogen using a mortar and pestle, and 15–20 mg was added to 500 μL homogenization buffer (5 mM EDTA, 50 mM HEPES, 0.1% Triton X-100, pH 7.4) for homogenization. The resulting slurry was centrifuged at 10,000 *G* for 2 min at 4 °C. 100 μL was then isolated for quantification of citrate synthase activity. Maximal enzyme activity was determined by the creation of 5-thio-2-nitrobenzoic acid (TNB) as a result of the reaction of acetyl CoA with 5,5′-dithiobis-2-nitrobenzoic acid (DTNB) at 412 nm at 25 °C for 10 min in triplicate. Enzyme well conditions were 50 mM Tris, pH 7.4, 0.5 mM oxaloacetate, 0.3 mM acetyl-CoA, 0.15 mM DTNB. Background absorption was measured prior to activity for 10 min and subtracted from the change in absorption when oxaloacetate was added. The extinction coefficient of 13.6 mM for TNB was used. Protein abundance of each sample was quantified using albumin standards (ThermoFisher) and a Bradford assay. For optimization, pilot assays were performed to determine the appropriate dilution for the greatest time over the linear portion of change in absorption. Maximal activity was normalized per gram of tissue and total soluble protein; however, data are presented here only as activity per mg of protein (μmol citrate mg protein^{-1} s^{-1}) since results of both were the same. We also report the average protein content per mg of tissue (μg mg^{-1}) for context.

2.5. Statistical analyses

All analyses were run in R (2022.02.03) using the packages *afex* (Singmann et al., 2015) and *emmeans* (Lenth et al., 2018) with an $\alpha = 0.05$. All data were tested for normality (Shapiro-Wilks Test) and homogeneity of the variance (Levene's Test) prior to analyses. Data that failed either of these assumptions were log10 transformed. All gene expression data were log10 transformed prior to analyses. Gene expression data were analyzed using type III sum-of-squares two-way ANOVAs with treatment (normoxia vs. hypoxia) and time point (1d, 4d, 8d) as factors, including interaction effects. When analyses showed significant interaction effects, Tukey post-hoc tests were conducted. Mitochondrial performance, citrate synthase activity, mass, relative ventricular mass, and Hct data were analyzed using Student's two-sample *t*-tests. Data are presented as averages ± s.e.m., unless otherwise noted.

3. Results

3.1. Gene expression

3.1.1. Heart

Relative *mb* expression significantly increased with hypoxia acclimation ($F_{1,27} = 4.98$, $p = 0.03$, $\eta^2 = 0.16$), but was not affected by time point ($F_{2,27} = 1.30$, $p = 0.29$). There was also no significant interaction between treatment and time point ($F_{2,27} = 1.31$, $p = 0.29$; Fig. 2A). Relative *cs* expression was not significantly affected by hypoxia acclimation ($F_{1,28} = 0.98$, $p = 0.33$) or time point ($F_{2,28} = 0.32$, $p = 0.73$), and there was no interaction effect ($F_{2,28} = 0.92$, $p = 0.41$; Fig. 2A).

3.1.2. Red muscle

Relative *cs* expression was also not affected by hypoxia acclimation ($F_{1,29} = 0.09$, $p = 0.77$) or time point ($F_{2,29} = 0.70$ $p = 0.50$), and there was no interaction effect ($F_{2,29} = 0.08$, $p = 0.92$; Fig. 2B). Relative *mb* expression was also unaffected by hypoxia acclimation ($F_{1,27} = 0.51$, $p = 0.23$) and time point ($F_{2,27} = 0.25$, $p = 0.78$), and there was no interaction effect ($F_{2,27} = 0.41$, $p = 0.67$; Fig. 2B).

3.1.3. Morphology and Hct

There were no significant differences between the masses of the normoxia-acclimated and hypoxia-acclimated individuals used for heart ($t = -1.7658$, df = 26, $p = 0.09$) or red muscle ($t = -1.2629$, df = 22, $p = 0.22$) mitochondrial performance and enzyme activity. Relative ventricular mass was not significantly affected by hypoxia acclimation among individuals used for heart (normoxia: 0.674 ± 0.021 mg/g, hypoxia: 0.672 ± 0.017 mg/g, $t = 0.060322$, df = 26, $p = 0.95$) or red muscle (normoxia: 0.620 ± 0.019 mg/g, hypoxia: 0.586 ± 0.025 mg/g; $t = -1.0705$, df = 22, $p = 0.30$) mitochondrial performance. Hct was significantly higher in hypoxia-acclimated individuals tested for heart (normoxia: 26.2 ± 0.7%, hypoxia: 28.5 ± 0.6%; $t = -2.4536$, df = 20, $p = 0.023$) and red muscle (normoxia: 30.2 ± 1.3%, hypoxia: 34.3 ± 1.1%; $t = 2.368$, df = 22, $p = 0.027$) mitochondrial performance.

3.2. Mitochondrial performance

3.2.1. Heart

There was no significant effect of hypoxia acclimation on CI-OXPHOS ($t = -0.7063$, df = 25, $p = 0.49$), LEAK ($t = -1.2483$, df = 24, p = 0.22; Fig. 3A), OXPHOS ($t = -0.0973$, df = 13, 0.92; Fig. 3B), or ETS ($t = -0.7784$, df = 13, $p = 0.45$; Fig. 3C). Hypoxia acclimation also did not significantly affect OXPHOS Capacity ($t = -0.0518$, df = 24, $p = 0.96$; Fig. 4A), Excess Capacity ($t = -0.0695$, df = 13, p = 0.95; Fig. 4B), ETS Capacity ($t = -0.46214$, df = 13, $p = 0.6516$), or RCR ($t = 0.5486$, df = 24, $p = 0.59$). OXPHOS Control Efficiency ($t = -0.8979$, df = 24, $p = 0.38$), OXPHOS CR ($t = -0.18805$, df = 25, $p = 0.85$; Fig. 4C), LEAK CR ($t = -0.4627$, df = 12, p = 0.65), CI Coupled CR ($t = -0.5965$, df = 25, 0.56), and CI Uncoupled ($t = -0.2792$, df = 13, $p = 0.79$) were also unaffected by hypoxia acclimation. Average ROX-corrected raw respiration rates and control ratios of cardiac muscle mitochondria can be found in Table 2.

3.2.2. Red muscle

LEAK ($t = 0.7833$, df = 22, $p = 0.44$; Fig. 3D), OXPHOS ($t = -1.641$, df = 22, $p = 0.11$; Fig. 3E), and ETS ($t = 0.0972$, df = 22, $p = 0.92$; Fig. 3F) were not significantly affected by hypoxia acclimation. However, there was a significant increase in OXPHOS Capacity of hypoxia-acclimated fish compared to control fish ($t = -2.4836$, df = 22, $p = 0.023$; Fig. 4D). Excess Capacity was also significantly decreased by hypoxia acclimation ($t = 2.6046$, df = 22, $p = 0.016$; Fig. 4E). OXPHOS Control Efficiency was significantly affected by hypoxia acclimation ($t = 2.2430$, df = 22, $p = 0.035$), such that hypoxia acclimated fish had a significantly higher OXPHOS Control Efficiency compared to normoxic fish. Additionally, OXPHOS CR was significantly affected by hypoxia acclimation ($t = -2.822$, df = 22, $p = 0.010$; Fig. 4F), such that hypoxia-acclimated fish had significantly higher CR than normoxia-acclimated fish. RCR was also significantly higher in hypoxia-acclimated fish ($t = -2.3802$, df = 22, $p = 0.026$). LEAK CR (t = −0.1880, df = 24, $p = 0.85$), CI-Coupled CR ($t = -0.0971$, df = 22, p = 0.92), and CI-Uncoupled CR (*t*

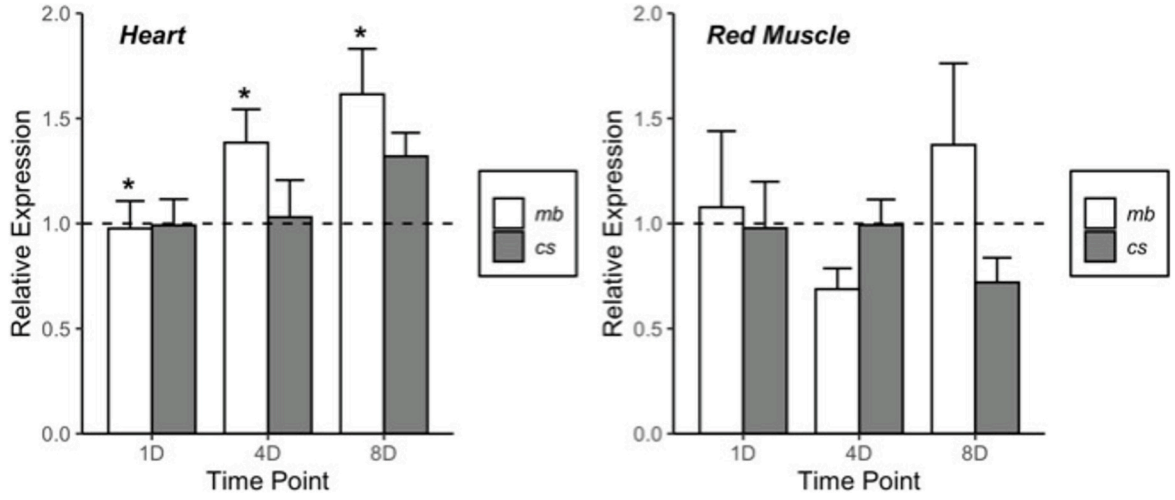

Fig. 2. Gene expression results for heart and red muscle tissues of hypoxia-acclimated red drum (*Sciaenops ocellatus*). Expression of each gene is normalized to the control gene, *ef1α*. The dotted line at 1.0 represents expression of normoxia-acclimated individuals. Only the expression levels for hypoxia-acclimated individuals are shown, and are relative to control within each time point (n = 6–8/treatment/timepoint) for (A) heart and (B) red muscle. Significant differences are denoted as follows: (*) indicates a main effect of hypoxia acclimation on gene expression. Values show are means ± s.e.m.; statistical outputs for these data are outlined in the text. (For interpretation of the references to colour in this figure legend, the reader is referred to the web version of this article.)

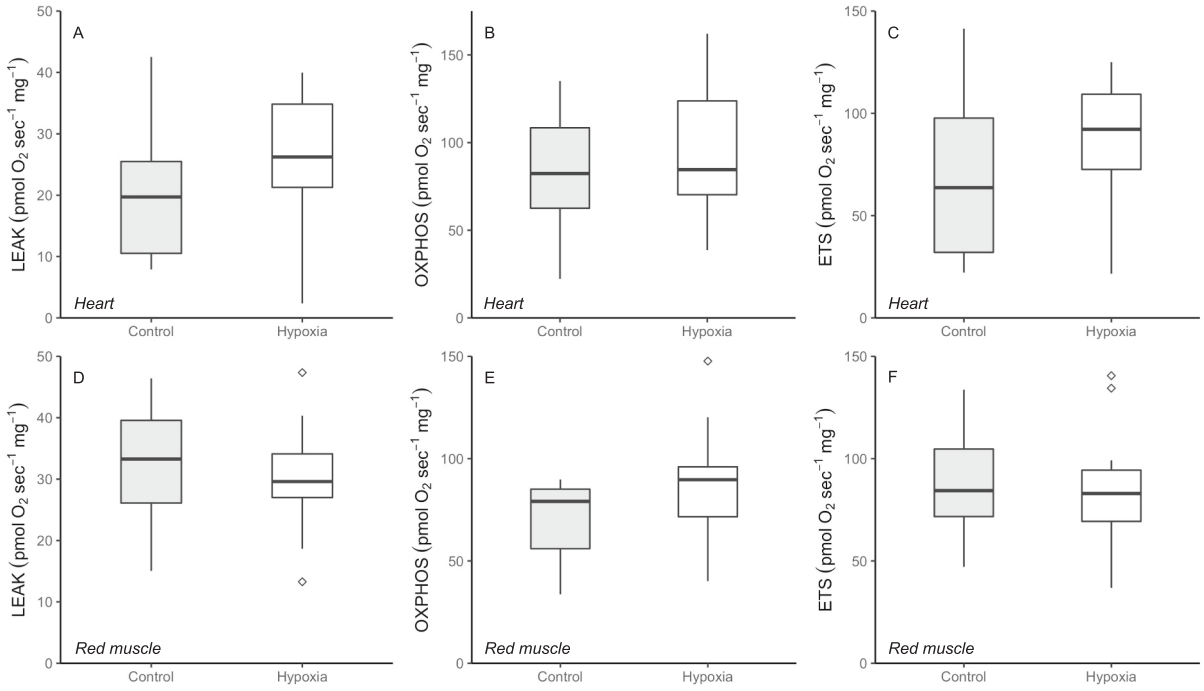

Fig. 3. Effects of hypoxia acclimation on raw mitochondrial respiration rates of red drum (*Sciaenops ocellatus*). Results of 8d chronic sub-lethal hypoxia acclimation on (A) proton leak (LEAK), (B) oxidative phosphorylation (OXPHOS), and (C) electron transport capacity (ETS) of red drum heart tissue (n = 14/treatment for LEAK, OXPHOS; n = 7–9/treatment for ETS) and (D) LEAK, (E) OXPHOS, and (F) ETS of red drum red muscle tissue (n = 12/treatment). Within the boxplots, the bold interior line represents the median, the edges are the interquartile range, and the whiskers are 1.5 of the interquartile range. Diamonds are points outside of this range, but are not statistical outliers. Statistical outputs for each parameter are outlined in the text. (For interpretation of the references to colour in this figure legend, the reader is referred to the web version of this article.)

= 0.1884, df = 22, p = 0.85) were not significantly affected by hypoxia acclimation. Additionally, ETS Capacity, (t = −0.49341, df = 22, p = 0.63), CI-OXPHOS (t = −1.594, df = 22, p = 0.13), and ETS (t = 0.0972, df = 22, p = 0.92) showed no significant differences between normoxia- and hypoxia-acclimated fish. Average ROX-corrected raw respiration rates and control ratios of red muscle mitochondria can be found in Table 2.

3.2.3. Citrate synthase activity

There was a significant increase in citrate synthase activity in the hearts of hypoxia-acclimated fish compared to control fish (t = −1.9067, df = 26, p = 0.034; Fig. 5A). In the heart, the average protein content in normoxia-acclimated fish was 39.78 ± 2.37 μg mg^{-1} and 41.42 ± 2.27 μg mg^{-1} in hypoxia-acclimated fish. Hypoxia acclimation did not significantly affect citrate synthase activity (t = −0.4843, df = 21, p = 0.32; Fig. 5B) in red muscle tissue. In the red muscle, the average protein

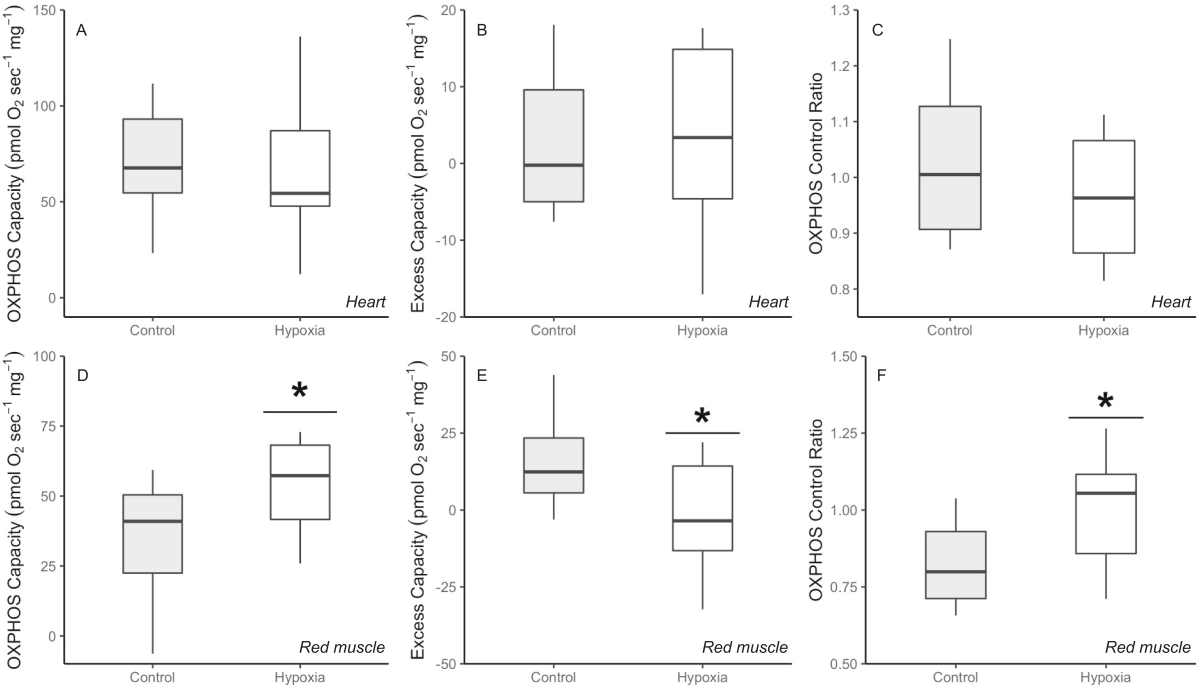

Fig. 4. Effects of hypoxia acclimation on mitochondrial performance of red drum (*Sciaenops ocellatus*). Results of 8d chronic sub-lethal hypoxia acclimation on Oxidative Phosphorylation (OXPHOS) Capacity, Excess Capacity, and OXPHOS Control Ratio (CR) on red drum heart tissue (A-C) ($n = 14$/treatment for OXPHOS Capacity; $n = 7$–9/treatment for Excess Capacity, OXPHOS CR) and (D—F) (red muscle tissue ($n = 12$/treatment). Asterisk (*) represents significant difference from control. Within the boxplots, the bold interior line represents the median, the edges are the interquartile range, and the whiskers are 1.5 of the interquartile range. Statistical outputs for each parameter are outlined in the text. (For interpretation of the references to colour in this figure legend, the reader is referred to the web version of this article.)

Table 2
ROX-corrected raw respiration rates and control ratios of mitochondria in red drum (*Sciaenops ocellatus*) acclimated to normoxic or hypoxic conditions. Values show means ± s.e.m. for cardiac (heart) and red muscle tissues of normoxia- and hypoxia-acclimated groups. Bolded values are significantly different from control (normoxia treatment). Statistical outputs for each parameter are outlined in the text.

	Heart		Red Muscle	
	Treatment		*Treatment*	
	Normoxia	Hypoxia	Normoxia	Hypoxia
CI-OXPHOS	63.50 ± 8.56	72.07 ± 8.57	41.80 ± 3.50	51.03 ± 4.63
OXPHOS	84.36 ± 9.58	95.58 ± 10.35	70.67 ± 5.53	86.97 ± 8.25
LEAK	20.08 ± 3.02	25.44 ± 3.02	36.38 ± 5.86	30.13 ± 2.66
ETS	70.23 ± 19.16	86.94 ± 10.58	87.19 ± 7.61	86.09 ± 8.42
OXPHOS Capacity	69.46 ± 7.95	70.14 ± 10.00	34.30 ± 5.2	**56.84 ± 7.19**
ETS Capacity	47.81 ± 13.72	55.14 ± 9.24	50.82 ± 8.12	55.96 ± 6.54
Excess Capacity	4.28 ± 3.43	3.29 ± 4.02	16.52 ± 4.48	**−0.88 ± 4.96**
OXPHOS Control Efficiency	0.76 ± 0.04	0.70 ± 0.05	0.48 ± 0.06	**0.64 ± 0.03**
RCR	5.52 ± 0.93	5.69 ± 1.55	2.20 ± 0.21	**3.02 ± 0.28**
OXPHOS CR	1.03 ± 0.06	1.04 ± 0.11	0.82 ± 0.04	**1.03 ± 0.07**
LEAK CR	0.36 ± 0.05	0.43 ± 0.10	0.43 ± 0.07	0.36 ± 0.02
CI COUPLED CR	0.74 ± 0.03	0.77 ± 0.05	0.59 ± 0.02	0.59 ± 0.02
CI UNCOUPLED CR	0.71 ± 0.07	0.74 ± 0.05	0.80 ± 0.02	0.80 ± 0.01

content in normoxia-acclimated fish was 39.92 ± 1.16 μg mg^{-1} and 41.78 ± 1.89 μg mg^{-1} in hypoxia-acclimated fish.

4. Discussion

Recent work from our group has documented a robust respiratory response to hypoxia in the estuarine-dependent red drum. While this response includes a typical increase in ventilation rate, amplitude, and minute volume (Ern and Esbaugh, 2016; Ern and Esbaugh, 2018), a more interesting phenomenon is the observed phenotypic plasticity that improves critical oxygen threshold (Pan et al., 2017), critical swim speed (Dichiera et al., 2022), maximum metabolic rate in hypoxia, and Hb-O_2 binding affinity (Negrete Jr et al., 2022). Following on these observations, we sought to expand our exploration of phenotypic plasticity following prolonged hypoxia exposure to mitochondrial respiratory, particularly those mitochondria found in the aerobic cardiac and red muscle. Interestingly, we observed different responses in the respective tissues, with only red muscle showing evidence of mitochondrial plasticity that would benefit performance in hypoxia.

We originally hypothesized that both red and cardiac muscle would respond to prolonged hypoxia acclimation by reducing LEAK respiration rates, as this represents the utilized oxygen that does not contribute to ATP generation. We saw no changes to raw LEAK respiration rates in either tissue, nor were changes in raw OXPHOS or ETS observed in either tissue (Fig. 3). However, the lack of statistically significant change belies an important improvement in red muscle mitochondrial efficiency whereby hypoxia-acclimated fish had significantly higher OXPHOS Control Efficiency (i.e., (OXPHOS – LEAK)/OXPHOS). This metric reflects the amount of oxygen being used to produce ATP relative to that lost to LEAK within a single sample. These data support our initial hypothesis, at least with respect to red muscle. It is also interesting to note that OXPHOS Capacity (i.e., OXPHOS-LEAK) (Fig. 4D) and RCR (OXPHOS/LEAK) were also elevated in red muscle following

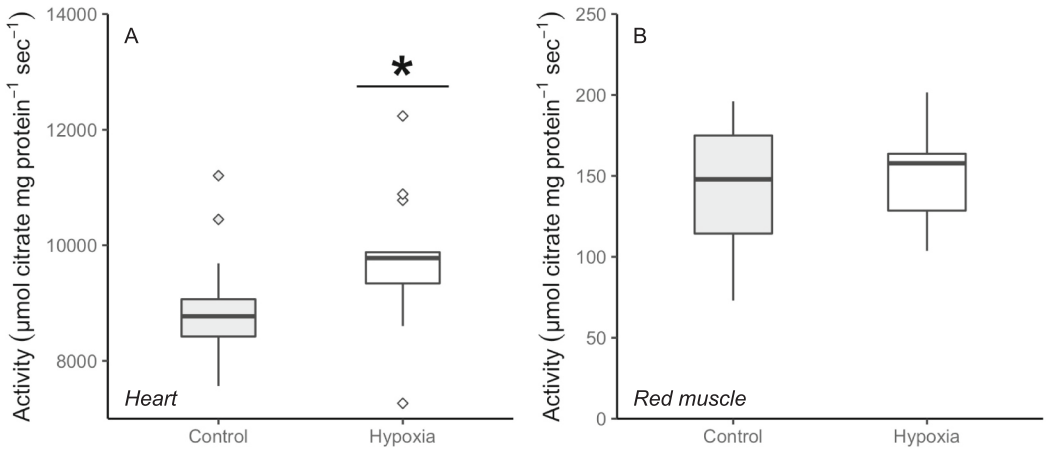

Fig. 5. Impact of 8d hypoxia acclimation on citrate synthase activity of red drum (*Sciaenops ocellatus*) cardiac and red muscle tissues. Results of 8d chronic sub-lethal hypoxia acclimation on (A) heart (n = 14) and (B) red muscle (n = 12) citrate synthase activity. Asterisk (*) represents significant difference from control. Within the boxplots, the bold interior line represents the median, the edges are the interquartile range, and the whiskers are 1.5 of the interquartile range. Diamonds are points outside of this range, but are not statistical outliers. Statistical outputs for each parameter are outlined in the text. (For interpretation of the references to colour in this figure legend, the reader is referred to the web version of this article.)

acclimation, which can be interpreted as an improved net ability to generate ATP. Taken together, these data suggest hypoxia-acclimated fish had significantly more efficient red muscle mitochondria and higher red muscle respiratory capacity compared to normoxia-acclimated fish.

It is also interesting to note that hypoxia-acclimated red muscle also had significantly reduced Excess Capacity (i.e., ETS-OXPHOS) and a significantly elevated OXPHOS CR (i.e., OXPHOS/ETS) (Fig. 4E,F). In fact, red muscle samples showed an average OXPHOS CR of 1, indicating mitochondria were working at maximum capacity and the phosphorylation system was limiting OXPHOS. Mitochondria from the red muscle of normoxia-acclimated fish were operating at ~80% of ETS. No hypoxia-induced changes were noted in the cardiac mitochondria; however, this may be in part due to the fact that these mitochondria were already working at maximum capacity even under normoxic conditions. While control ratios approaching 1 may appear unusual when compared to mammalian data, fishes do not rely on mitochondrial uncoupling for thermogenesis (see review by Mozo et al., 2005). In fact, our data are similar to a previous study of red drum cardiac and red muscle permeabilized fibres (Johansen and Esbaugh, 2017), and such high control ratios can also be corroborated by studies in other fish species (Dos Santos et al., 2012; Du et al., 2016). Most importantly, these data support the notion that mitochondrial efficiency in both tissues is maximized under hypoxia.

In addition to mitochondrial respiration rates, which provide a tissue wide assessment of mitochondrial function, we also assessed citrate synthase activity and gene expression as a measure of mitochondrial density. Interestingly, citrate synthase activity was only elevated in cardiac muscle following hypoxia acclimation (Fig. 5A). Despite the discrepancy between gene expression and enzyme activity – a finding that is not altogether unusual – these data suggest that changes in red muscle mitochondrial respiration characteristics are not the result of mitochondrial biogenesis. Furthermore, the observed changes in cardiac citrate synthase in the absence of improved OXPHOS are indicative of reduced OXPHOS rates when normalized for mitochondrial density (i.e., OXPHOS per µmol citrate s^{-1}). This counterintuitive finding may be indicative of a not fully acclimated phenotype, whereby cardiac muscle may be actively increasing mitochondrial density but these mitochondria are not effectively contributing to an improved OXPHOS. While the length of our acclimation was based on two prior 42 day time trial studies in red drum that demonstrated that transcriptional changes were largely complete by 8 days of acclimation, which were also coincident with phenotypic changes includes U_{crit}, P_{crit}, MMR in hypoxia and Hb-O_2 binding affinity (Dichiera et al., 2022; Negrete Jr et al., 2022; Pan et al., 2017). While we cannot say whether a longer duration would improve OXPHOS, it is clear that our data generally aligns with previous work in other fishes, including goldfish (Farhat et al., 2021), epaulette shark (Hickey et al., 2012), snapper (*Pagrus auratus*) (Cook et al., 2013), and sablefish (Gerber et al., 2019). In these species hypoxia did not significantly affect mitochondrial respiration rates of the cardiac tissue, although a 20% increase in citrate synthase activity in cardiac tissue was observed in sablefish (Gerber et al., 2019). Though we did not measure reactive oxygen species (ROS) within this experiment, previous work in fishes has shown changes to ROS production following exposure to hypoxia, though it often depends on the hypoxia-tolerance of the species (e.g., Du et al., 2016; Gerber et al., 2019; Hickey et al., 2012). Therefore, this limited OXPHOS response could also be a protective measure to prevent generation of ROS with higher rates of ETS that may result in cellular damage and warrants further investigation. Interestingly, Cook et al. (2013) did find that while snapper cardiac tissue maintained mitochondrial respiration rates under hypoxia, the mitochondria became more effective at O_2 uptake with a lower mitochondrial P_{50}. Thus, mitochondrial P_{50} may be an intriguing next step to further assess changes in mitochondrial function in cardiac tissues.

A last measure that was assessed in our experiment was myoglobin transcript abundance (Fig. 2). While not directly related to mitochondrial performance, myoglobin is important for both intracellular O_2 storage and facilitated diffusion that aids in transporting O_2 through the cytoplasm to mitochondria. Due to limited sample mass, we were unable to validate the transcriptional responses at the phenotype level, so these data must be viewed with some caution. Nonetheless, we saw no change to *mb* expression in red muscle between treatments, though we had predicted an increase in *mb* expression to support increased OXPHOS. In contrast, cardiac muscle had significantly higher *mb* expression following hypoxia-acclimation. This may suggest that cardiac muscle is actively working to prevent O_2 limitations at the site of the mitochondria, either by augmenting intracellular O_2 reserves or improving O_2 diffusion rates through the cell. Though previous work exploring *mb* expression in fishes under hypoxia is variable, our findings do align with data from zebrafish (*Danio rerio*), which found mildly increased *mb* expression in cardiac tissue of individuals exposed to hypoxia (Roesner et al., 2006), as well as previous work in crucian carp (*Carassius carassius*), which found no significant increase in *mb* expression in red muscle as a result of hypoxia (Hansen et al., 2016).

At this point it is important to acknowledge two short comings of the current work. The first is that cardiac tissues samples and red muscles samples were taken from different individuals of different sizes. This was the unfortunate result of the fact that the red muscle samples taken alongside the cardiac samples in the smaller fishes were not large enough to obtain high quality mitochondrial data. As such, the experiment was repeated with larger fish focusing only on the red muscle. It is important to note that no cross-tissue comparisons were performed here, and all treatment fish were compared to size matched control fish. A second concern is the observed stimulatory effect of externally added cytochrome *c* on OXPHOS. Here, we quantified mitochondrial respiration using a standard SUIT protocol using homogenized cardiac and red muscle tissue preparations. These in-situ assays are performed under ideal conditions (e.g., unlimited substrates, high O_2 levels) to measure maximal mitochondrial respiration. The tissue preparations (e.g., Salin et al., 2016) and SUIT protocol (Johansen and Esbaugh, 2017) used in this study have been previously validated in fishes, including the use of oligomycin to inhibit F_0F_1-ATPase to quantify LEAK respiration rates and FCCP to quantify uncoupled respiration rates (e.g., Fangue et al., 2009; Strobel et al., 2013). In regards to the tissue preparations, while isolated mitochondria and permeabilized fibres are more standard for these types of analyses, the homogenate approach used here has become more common (e.g., Salin et al., 2016). In fact, our data are remarkably similar to the respiration rates we previously presented for red drum permeabilized fibres (Johansen and Esbaugh, 2017), suggesting that tissue homogenates are an effective method for analysis of mitochondrial respiration in red drum. Nonetheless, it is important to note that the use of tissue homogenates does have drawbacks, as the presence of tissue can introduce non-mitochondrial O_2 consumption (e.g., oxidases) and interference from non-mitochondrial membrane proteins that can impact respiration rates. However, our results may suggest that red muscle preparations had some level of reduced outer membrane integrity. While hard and fast thresholds are not readily available for fishes, particularly for red muscle homogenate preparations, it is important to note that both treatments showed statistically similar levels of cytochrome *c* stimulation. The raw respiration rates and CRs also align with previous work by Johansen and Esbaugh (2017) on permeabilized red muscle fibres of red drum using an identical SUIT protocol. Additionally, within this SUIT protocol, OXPHOS, LEAK, and ETS respiration rates are quantified following the addition of cytochrome *c* – meaning respiration rates were measured in the presence of cytochrome *c*. While we cannot say for certain that the cytochrome *c* concentrations added were saturating – as the significant effect was only noted after the preparation was completed and fully analyzed – the consistency between treatments and the similarity to prior data from red drum red muscles provides a strong level of confidence in our conclusions.

Overall, our results show that red drum have the dynamic ability to acclimate to prolonged environmental hypoxia to maintain and improve aerobic performance through mitochondrial plasticity. While hypoxic responses are tissue-specific, as has been seen in other species, the data presented here show that red drum acclimated to 8 days of prolonged environmental hypoxia improve the efficiency of O_2 utilization in red muscle. Interestingly, these data may also help explain a confounding finding from our prior work in red drum. Dichiera et al. (2022) showed that red drum acclimated to 8 days of hypoxia improved U_{crit} without any improvement to MMR in swim tests performed in normoxia. Interestingly, MMR was improved when tested in hypoxia (Negrete Jr et al., 2022). Our data may help to explain these observations as, if in vitro predicts in vivo, acclimated individuals should produce more ATP in their swimming muscles per unit O_2 consumed. As such, red drum appear to both alter respiratory characteristics that benefit O_2 uptake – namely Hb isoform switching that coincides with improved Hb-O_2 binding affinity and reduced pH sensitivity – and improve the efficiency of O_2 utilization in aerobically powered swimming muscle.

Contributions

AJE, KLA, BNJ, and AMD conceptualized the project, and AJE supervised the project. KLA, BNJ, and AMD performed all of the hypoxia acclimations. KLA, BNJ, and AMD collected the samples for gene expression, and AMD conducted mRNA extract and cDNA synthesis for qPCR experiments. KLA conducted the gene expression experiments, including primer design and verification. KLA did all of the dissections, preparations, experiments, and analyses for mitochondrial respiration experiments. BNJ conducted citrate synthase activity assays. KLA and BNJ performed formal statistical analyses and data visualization. KLA wrote the initial draft of the manuscript and all authors edited it.

Declaration of Competing Interest

The authors have no competing interests to declare.

Data availability

Data will be made available on request.

Acknowledgements

This research was funded by a grant from the National Science Foundation awarded to AJE (#2002549). BNJ was funded by the National Science Foundation Graduate Research Fellowship Program (#1610403). AMD was funded by the University of Texas at Austin Stengl-Wyer Graduate Fellowship.

References

Ackerly, K.L., Esbaugh, A.J., 2020. The additive effects of oil exposure and hypoxia on aerobic performance in red drum (Sciaenops ocellatus). Sci. Total Environ. 737, 140174.
Ackerly, K.L., Esbaugh, A.J., 2021. The effects of temperature on oil-induced respiratory impairment in red drum (*Sciaenops ocellatus*). Aquat. Toxicol. 233, 105773.
Brand, M.D., 2005. The efficiency and plasticity of mitochondrial energy transduction. Biochem. Soc. Trans. 33 (5), 897–904.
Buck, L.T., Pamenter, M.E., 2006. Adaptive responses of vertebrate neurons to anoxia—matching supply to demand. Respir. Physiol. Neurobiol. 154 (1–2), 226–240.
Chance, B., Williams, G.R., 1955. Respiratory enzymes in oxidative phosphorylation: III. The steady state. J. Biol. Chem. 217 (1), 409–427.
Chapman, L.J., Mckenzie, D.J., 2009. Behavioral responses and ecological consequences. In: Fish Physiol, vol. 27. Academic Press, pp. 25–77.
Cook, D.G., Iftikar, F.I., Baker, D.W., Hickey, A.J., Herbert, N.A., 2013. Low-O2 acclimation shifts the hypoxia avoidance behaviour of snapper (*Pagrus auratus*) with only subtle changes in aerobic and anaerobic function. J. Exp. Biol. 216 (3), 369–378.
Diaz, R.J., 2001. Overview of hypoxia around the world. J. Environ. Qual. 30 (2), 275–281.
Diaz, R.J., Rosenberg, R., 2008. Spreading dead zones and consequences for marine ecosystems. Science 321 (5891), 926–929.
Dichiera, A.M., Negrete Jr., B., Ackerly, K.L., Esbaugh, A.J., 2022. The role of carbonic anhydrase-mediated tissue oxygen extraction in a marine teleost acclimated to hypoxia. J. Exp. Biol. 225 (21) jeb244474.
Dos Santos, R.S., Galina, A., Da-Silva, W.S., 2012. Cold acclimation increases mitochondrial oxidative capacity without inducing mitochondrial uncoupling in goldfish white skeletal muscle. Biol. Open 2 (1), 82–87.
Du, S.N., Mahalingam, S., Borowiec, B.G., Scott, G.R., 2016. Mitochondrial physiology and reactive oxygen species production are altered by hypoxia acclimation in killifish (*Fundulus heteroclitus*). J. Exp. Biol. 219 (8), 1130–1138.
Ern, R., Esbaugh, A.J., 2016. Hyperventilation and blood acid–base balance in hypercapnia exposed red drum (*Sciaenops ocellatus*). Comp. Biochem. Physiol. B 186, 447–460.
Ern, R., Esbaugh, A.J., 2018. Effects of salinity and hypoxia-induced hyperventilation on oxygen consumption and cost of osmoregulation in the estuarine red drum (*Sciaenops ocellatus*). Comp. Biochem. Physiol. A Mol. Integr. Physiol. 222, 52–59.
Fangue, N.A., Richards, J.G., Schulte, P.M., 2009. Do mitochondrial properties explain intraspecific variation in thermal tolerance? J. Exp. Biol. 212 (4), 514–522.
Farhat, E., Cheng, H., Romestaing, C., Pamenter, M., Weber, J.M., 2021. Goldfish response to chronic hypoxia: mitochondrial respiration, fuel preference and energy metabolism. Metabolites 11 (3), 187.
Gerber, L., Clow, K.A., Katan, T., Emam, M., Leeuwis, R.H., Parrish, C.C., Gamperl, A.K., 2019. Cardiac mitochondrial function, nitric oxide sensitivity and lipid composition following hypoxia acclimation in sablefish. J. Exp. Biol. 222 (22) jeb208074.

Hansen, M.N., Lundberg, J.O., Filice, M., Fago, A., Christensen, N.M., Jensen, F.B., 2016. The roles of tissue nitrate reductase activity and myoglobin in securing nitric oxide availability in deeply hypoxic crucian carp. J. Exp. Biol. 219 (24), 3875–3883.
Hickey, A.J., Renshaw, G., Speers-Roesch, B., Richards, J.G., Wang, Y., Farrell, A.P., Brauner, C.J., 2012. A radical approach to beating hypoxia: depressed free radical release from heart fibres of the hypoxia-tolerant epaulette shark (*Hemiscyllum ocellatum*). Comp. Biochem. Physiol. B 182 (1), 91–100.
Johansen, J.L., Esbaugh, A.J., 2017. Oil-induced responses of cardiac and red muscle mitochondria in red drum (*Sciaenops ocellatus*). Comp. Biochem. Physiol. C Toxicol. Pharma. 219, 35–41.
Jorgensen, S.M., Kleveland, E.J., Grimholt, U., Gjoen, T., 2006. Validation of reference genes for real-time polymerase chain reaction studies in Atlantic salmon. Mar. Biotechnol. 8, 398–408.
Lenth, R., Singmann, H., Love, J., Buerkner, P., Herve, M., 2018. Emmeans: Estimated Marginal Means, Aka Least-Squares Means. R Package Version 1, p. 3.
Levin, L.A., Ekau, W., Gooday, A.J., Jorissen, F., Middelburg, J.J., Naqvi, S.W.A., Zhang, J., 2009. Effects of natural and human-induced hypoxia on coastal benthos. Biogeosciences 6 (10), 2063–2098.
Mozo, J., Emre, Y., Bouillaud, F., Ricquier, D., Criscuolo, F., 2005. Thermoregulation: what role for UCPs in mammals and birds? Biosci. Rep. 25 (3–4), 227–249.
Negrete Jr., B., Ackerly, K.L., Dichiera, A.M., Esbaugh, A.J., 2022. Respiratory plasticity improves aerobic performance in hypoxia in a marine teleost. e 157880.
Negrete Jr., B., Esbaugh, A.J., 2019. A methodological evaluation of the determination of critical oxygen threshold in an estuarine teleost. Biol. Open 8 (11), bio045310.
Pamenter, M.E., 2014. Mitochondria: a multimodal hub of hypoxia tolerance. Can. J. Zool. 92 (7), 569–589.
Pan, Y.K., Ern, R., Morrison, P.R., Brauner, C.J., Esbaugh, A.J., 2017. Acclimation to prolonged hypoxia alters hemoglobin isoform expression and increases hemoglobin oxygen affinity and aerobic performance in a marine fish. Sci. Rep. 7 (1), 1–11.
Pfaffl, M.W., 2001. A new mathematical model for relative quantification in real-time RT–PCR. Nucleic Acids Res. 29 (9) e45-e45.
Rabalais, N.N., Turner, R.E., 2019. Gulf of Mexico hypoxia: past, present, and future. Limnol. Oceanogr. Bull. 28 (4), 117–124.
Roesner, A., Hankeln, T., Burmester, T., 2006. Hypoxia induces a complex response of globin expression in zebrafish (*Danio rerio*). J. Exp. Biol. 209 (11), 2129–2137.
Salin, K., Villasevil, E.M., Auer, S.K., Anderson, G.J., Selman, C., Metcalfe, N.B., Chinopoulos, C., 2016. Simultaneous measurement of mitochondrial respiration and ATP production in tissue homogenates and calculation of effective P/O ratios. Phys. Rep. 4 (20), e13007.
Schmidtko, S., Stramma, L., Visbeck, M., 2017. Decline in global oceanic oxygen content during the past five decades. Nature 542 (7641), 335–339.
Singmann, H., Bolker, B., Westfall, J., Aust, F., 2015. afex: Analysis of Factorial Experiments. R Package Version 0.13–145.
Sokolova, I.M., Sokolov, E.P., Haider, F., 2019. Mitochondrial mechanisms underlying tolerance to fluctuating oxygen conditions: lessons from hypoxia-tolerant organisms. Integr. Comp. Biol. 59 (4), 938–952.
Strobel, A., Graeve, M., Poertner, H.O., Mark, F.C., 2013. Mitochondrial acclimation capacities to ocean warming and acidification are limited in the Antarctic nototheniid fish, Notothenia rossii and Lepidonotothen squamifrons. PLoS One 8 (7), e68865.
Watson, C.J., Nordi, W.M., Esbaugh, A.J., 2014. Osmoregulation and branchial plasticity after acute freshwater transfer in red drum, Sciaenops ocellatus. Comp. Biochem. Physiol. A Mol. Integr. Physiol. 178, 82–89.
Yang, C.G., Wang, X.L., Tian, J., Liu, W., Wu, F., Jiang, M., Wen, H., 2013. Evaluation of reference genes for quantitative real-time RT-PCR analysis of gene expression in Nile tilapia (*Oreochromis niloticus*). Gene 527 (1), 183–192.